Structures 25 (2020) 147–156

Contents lists available at ScienceDirect

Structures

journal homepage: www.elsevier.com/locate/structures

Proposed design procedure for steel self-centring tension-only braces with resilient connections

Ashkan Hashemi[a,*], George Charles Clifton[a], Hamed Bagheri[a], Pouyan Zarnani[b], Pierre Quenneville[a]

[a] Department of Civil and Environmental Engineering, Faculty of Engineering, The University of Auckland, Private Bag 92019, Auckland 1142, New Zealand
[b] Department of Built Environment Engineering, School of Engineering, Computer and Mathematical Sciences, Auckland University of Technology, Private Bag 92006, Auckland 1142, New Zealand

ARTICLE INFO

Keywords:
Low damage
Tension-only
Friction
Self-centring
Steel braces
Resilience

ABSTRACT

While conventional steel seismic resistant structural systems may provide sufficient safety for the occupants, generally they depend on damage in the selected structural members to resist severe earthquakes. Therefore, after such an event, there may be considerable economic loss and significant repairs followed by business downtime. In addition, the post-event residual displacement of the structure can compromise the post-disaster functionality of the building. Recent severe earthquakes in New Zealand have highlighted the problems with assessment and repair or replacement of buildings designed for controlled damage and have provided a strong motivation for researchers and engineers to start developing concepts and design methods for low damage self-centring systems.

This paper proposes a step-by-step design procedure for steel braced frames with diagonal tension-only braces equipped with the innovative Resilient Slip Friction Joint (RSFJ) connections. The proposed procedure is used to design a 5-story steel structure with RSFJ tension-only x-braces to verify its efficiency and to demonstrate that the system can meet the ductility demand recommended by the standard. The numerical results showed that the proposed procedure could accurately predict the behaviour of the system and potentially can be used for low damage bracing systems with a flag-shaped load-deformation response.

1. Introduction

Following the Canterbury earthquake sequence (2010 to 2012) in New Zealand, it was observed that the steel structures have performed very well, considering the severity of the seismic events, most particularly structures with seismic resisting systems such as Eccentrically Braced Frames (EBFs) or Concentrically Braced Frames (CBFs) [1]. However, the structures were designed for the 'life-safety' criteria so post-disaster repair costs (if the structure is repairable) and the associate business downtime have significantly affected the economy of the recovering city. Moreover, the previous studies have demonstrated that residual drifts more than 0.3% can impact on the structural functionality and more than 0.5% require realignment which is difficult and would probably result in building replacement. Even residual drifts of 0.15% will require realignment of lift shaft guide rails, involving significant cost and disruption [2]. Furthermore, McCormick et al. [3] asserted to the fact that a residual drift of 0.5% is an important index in terms of permissible residual displacements.

With the growing acknowledgement of the post-event economic impacts on society has come the increased demand for low damage systems that can deliver a high resistance level against the severe earthquakes. These systems allow buildings to be rapidly returned to service, with negligible or no residual displacement and requiring maintenance which can be delayed and undertaken at a time to suit the client.

The use of friction connections to dissipate the earthquake energy and reduce the induced damage dates back to 1980s where Pall et al. [4–6] proposed the use of friction joints in panel-to-panel connections and steel braces. Later, Popov et al. proposed the use of friction connections in the beam-column joints in steel moment frames [7]. Clifton et al. [8] introduced the Sliding Hinge Joint (SHJ) that was an innovative friction-based energy dissipation concept specifically designed and configured for steel moment resisting frames. Bora et al. [9] used symmetric friction connections as hold-downs for reinforced concrete

* Corresponding author.
E-mail addresses: ahas439@aucklanduni.ac.nz (A. Hashemi), c.clifton@auckland.ac.nz (G.C. Clifton), hbag051@aucklanduni.ac.nz (H. Bagheri), pouyan.zarnani@aut.ac.nz (P. Zarnani), p.quenneville@auckland.ac.nz (P. Quenneville).

https://doi.org/10.1016/j.istruc.2020.02.024
Received 20 January 2020; Received in revised form 19 February 2020; Accepted 26 February 2020

shear walls. Loo et al. [10] adopted a similar concept and used friction connections as hold-downs for rocking timber shear walls. Dal Lago et al. [11] experimentally investigated the application of friction-based dissipative devices for rocking precast concrete coupled walls. Hashemi et al. investigated the use of friction connections in timber jointed wall systems [12,13].

In the studies mentioned, a high level of energy dissipation with minimum damage was observed. That is the reason why friction joints are known as one of the most efficient damping systems. Nevertheless, in many of the studies, significant amounts of residual displacements was observed [12,14] and it was shown that for most of the friction systems, an additional mechanism (such as the gravity loads from the building [10] or pre-tensioned elements [15–17]) may be required to provide a self-centring structural system.

The Resilient Slip Friction Joint (RSFJ) technology [18] is a recently developed friction-based structural low damage technology that has already been implemented in real projects. This technology provides self-centring behaviour and seismic energy dissipation in one package. It also includes a built-in collapse prevention secondary fuse function that adds more resilience to the system in case of a seismic event larger than the design level. Hashemi et al. [19,20] experimentally verified the flag-shaped hysteresis and the self-centring characteristic of the RSFJ.

Fig. 1 shows the components and the assembly of the RSFJ. In this joint, the energy is dissipated by frictional sliding of the moving plates while the specific shape of the ridges combined with the use of disc springs provide the necessary self-centring behaviour. At the time of unloading, the restoring force induced by the elastically compacted disc springs is greater than the resisting frictional force between the sliding parts. Thus, the elastic force in the discs re-centres the middle plates to their original stationary position. Fig. 1(c) shows the device at rest when the disc springs are partially compacted. When the force applied to the joint overcomes the resistance between the clamped plates, the middle plates start to move, and the cap plates start to laterally expand until the joint is at the maximum deflection and the discs are flat (see Fig. 1(d)).

Fig. 1(b) displays the load-deformation behaviour for the RSFJ. The slip force (F_{slip}) and the residual force ($F_{residual}$) in the joint can respectively be determined by Eqs. (1) and (2) where $F_{b,pr}$ is the clamping force in the bolts, n_b is the number of bolts, θ is the angle of the ridges, μ_s is the static coefficient of friction and μ_k is the kinetic coefficient of friction. The ultimate force in loading ($F_{ult,loading}$) and unloading ($F_{ult,unloading}$) can be calculated by substituting μ_s and $F_{b,pr}$ in Eqs. (1) and (2) with μ_k and $F_{b,u}$, respectively. It should be noted that the initial stiffness of the RSFJ (the stiffness before F_{slip} in Fig. 1(b)) is related to elastic stiffness of the sliding plates and of any other component connected to the RSFJ.

$$F_{slip} = 2n_b F_{b,pr}\left(\frac{sin\theta + \mu_s cos\theta}{cos\theta - \mu_s sin\theta}\right) \quad (1)$$

$$F_{residual} = 2n_b F_{b,pr}\left(\frac{sin\theta - \mu_k cos\theta}{cos\theta + \mu_k sin\theta}\right) \quad (2)$$

The reader is referred to [21,22] for more information about the full-scale experimental tests that have been conducted on different applications of the RSFJs, including the test results and discussions.

2. Steel tension-only braces with RSFJs

Fig. 2 schematically shows the RSFJ tension-only concept. In this concept, the RSFJ device is in series with the diagonal tension members forming an x-braced system effective in tension only so there will be no global buckling in the brace bodies. Rebars, threaded rods, flat steel plates or any other type of tension-only element can be considered for the diagonal members. As can be seen in the figure, multiple diagonal members with multiple RSFJs can also be used if required.

In this concept, RSFJs provide the required seismic performance (flag-shaped load-deformation behaviour) as the weak links in the system. Thus, the diagonal members are capacity designed with an appropriate over-strength factor to remain elastic. The appropriate over-strength factor to be considered for designing the diagonal members, connections and gusset plates is discussed in the next section. Note that in this concept, there is no buckling demand on the gusset plates so they can be designed for tension only.

Bagheri et al. [23] performed full scaled dynamic tests on a steel braced frame with RSFJ tension-only braces. The experimental results confirmed the low damage performance of the system with repeatable flag-shaped load-deformation curves. A fully self-centring behaviour was observed for the frame. Furthermore, the hysteretic performance of this system was similar to a system with tension/compression braces that have equal strength and stiffness in both directions of loading in the plane of the frame. The reader is referred to [23] for more information about the tests including results and discussions.

3. The proposed design procedure for the RSFJ tension-only braces

In this section, a design procedure is proposed and then implemented for the design of a multi-storey case study steel structure with RSFJ tension-only braces as its primary seismic resisting system.

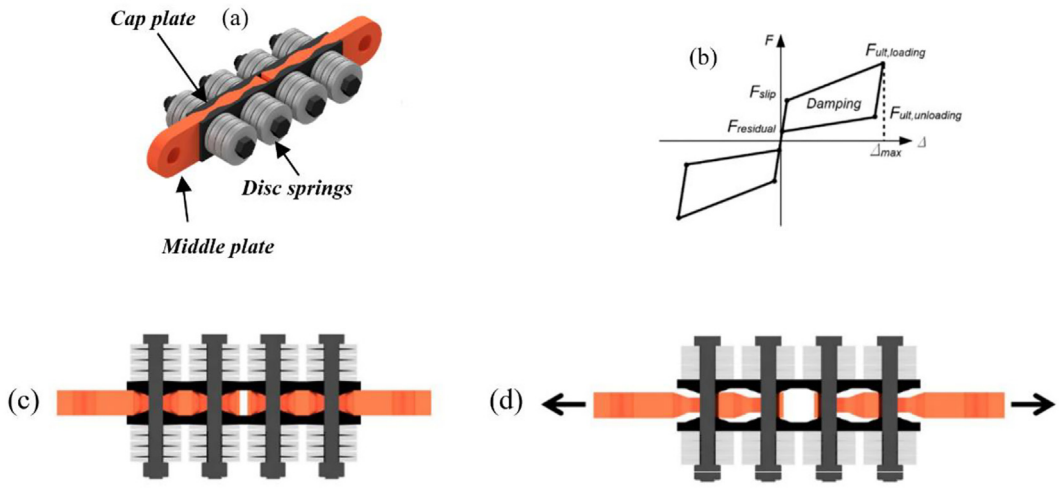

Fig. 1. Resilient Slip Friction Joint (RSFJ): (a) assembly (b) hysteresis (c) the joint at rest (d) the joint at the maximum deflection.

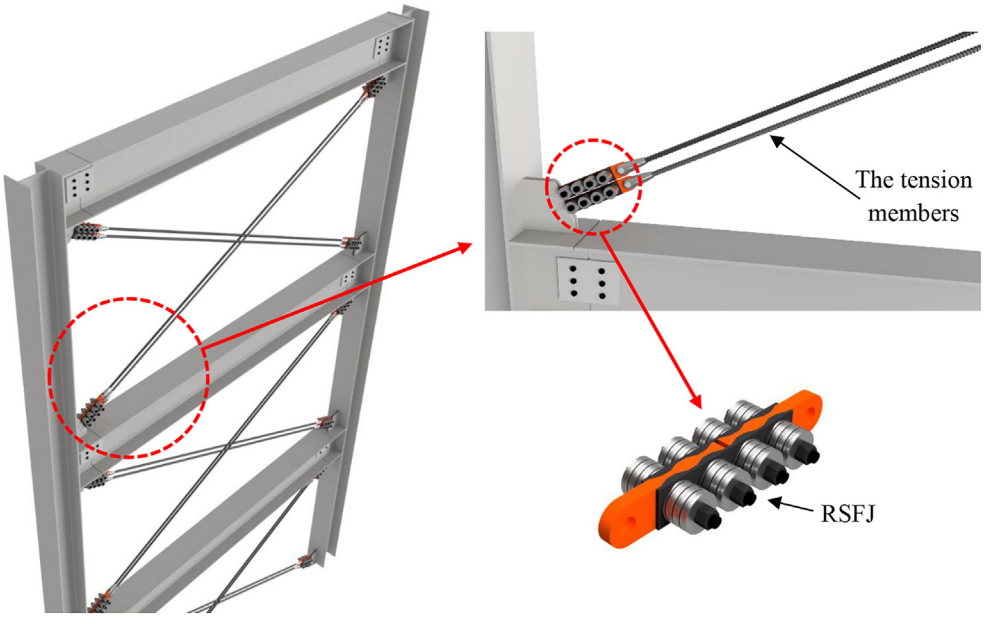

Fig. 2. The concept of steel tension-only brace with RSFJs.

The proposed design procedure is based on the New Zealand standard for steel structures [24] and the design procedures recommended by the Heavy Engineering Research Association (HERA) [25] for CBFs with modifications to account for the characteristics of the RSFJ tension-only brace. This report forms the basis of current steel seismic design practice in New Zealand (in which the concepts are similar to the other international building standards) meaning that designers are more than likely familiar with the procedures involved. The column splice provisions of New Zealand Standard for Steel Structures [24] are applied to all columns in the structure, not just the seismic resisting system ones, to ensure that the gravity system columns are continuous over the height of the structure. This is to meet the additional focus on structural system ductility recommended after the Canterbury earthquakes [1].

The design force for all structural members in this example is determined using the Equivalent Static Method (ESM) described in [26] which is a Forced-Based Design (FBD) method. The Modal Response Spectrum Analysis Method (RSA) would have been equally applicable.

The following section describes the general arrangement of the example structure that the proposed procedure is applied to. The sections after that describes the preliminary design procedure and the procedure used to specify the member sizes.

3.1. The example case-study structure

The general configuration of the considered case study structure is shown in Fig. 3. The five-storey building is 18 m tall and is symmetrical about the two main axes. Along each axis, RSFJ tension-only braces are used as the Lateral Load Resisting Systems (LLRSs). The brace arrangement is symmetrical to fulfil the condition required by [26] where the difference in the brace forces should not exceed 20%. Respecting the symmetrical configuration of the braced bays, it can be concluded that each braced frame resists half of the lateral seismic loads, ignoring accidental eccentricity which is appropriate for this design example but must be considered in practice. The structure is composed of steel frames with composite floor slabs. It was assumed that this building is located at Christchurch with a Class D soil type and a Hazard factor of $Z = 0.3$. The building is an office-type building thus it has an importance level of 2 and is designed for a working life of 50 years. This building has only two seismic resisting systems in each direction and won't meet the latest proposed changes to NZS1170.5 for redundancy. However, this doesn't detract from its usefulness as a design example. Keeping this layout and making the gravity columns continuous would meet the intent of these provisions rather than adding a third seismic resisting system in each direction.

3.2. The design procedure

The proposed design procedure has two parts. The first part presents the preliminary design of the structure, while the second part focuses on the design of the members. The RSFJ tension-only brace system can be classified either as a fully ductile (category 1 [24]) or limited ductile system (category 2 [24]) depending on the adopted ductility factor and detailing of the structure. In other words, it has been confirmed that the RSFJ technology is scalable and can be tuned based the design requirements [27]. However, other aspects of the design should also be addressed for the whole system to be considered as a fully ductile system or a system with limited ductility.

3.2.1. The preliminary design

3.2.1.1. Step 1: check that the maximum height limitation is satisfied. The first step to design a braced frame is to check whether a maximum height limitation is required and, if so, whether it is satisfied. According to [24], the tension-braced CBF systems are permitted only in x-braced systems up to two storeys. However, the experimental test of Bagheri et al. [23] on full-scale RSFJ tension-only braced frames showed that the performance of this system (load-deformation behaviour) in terms of retention of strength and stiffness under reversing loading is as good as that of a system with braces effective in tension and compression and with a brace slenderness ratio ≤ 30. Thus, for a category 2 system (similar to the design example here) a height limit of 12 storeys applies from [24] Table 12.12.4(2). This is similar to the recommendations of Wijanto [28] for designing a CBF system with Buckling Restrained Braces (BRBs). However, the RSFJ tension only system has the additional advantage of active self-centring.

3.2.1.2. Step 2: determine the design seismic load incorporating the factor C_S. Clause 12.12.3 of [24] requires the application of a C_s factor to account for the less desirable inelastic response of capacity designed CBF systems in general compared with that of capacity designed MRF or EBF systems. However, the C_s factors in this clause are developed for conventional braced systems, using the procedure given in the commentary clause C12.12.3. The C_s factor in the standard is the

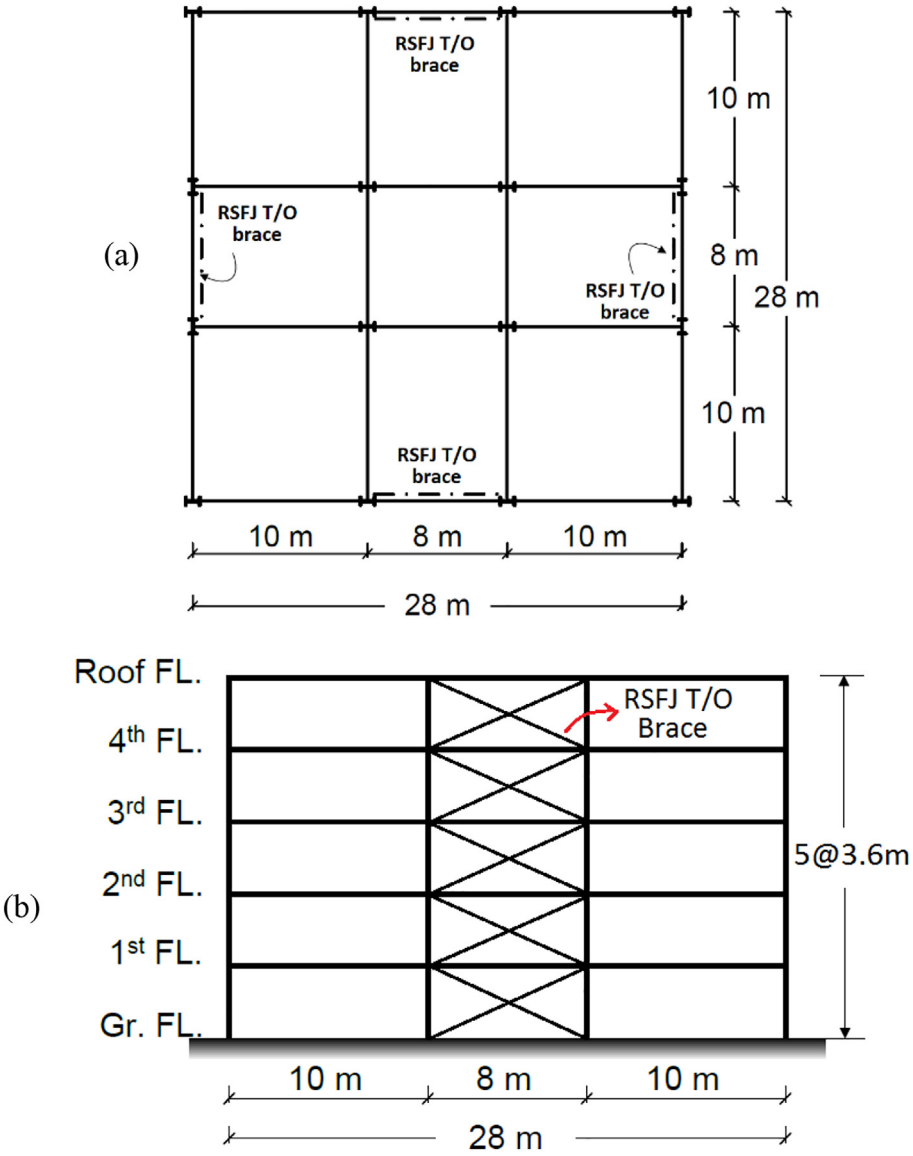

Fig. 3. General configuration of the case study structure: (a) plan view (b) elevation view.

product of three variables *A*, *B* and *C*.

To determine the appropriate C_s factor for the RSFJ tension only system, the commentary procedure needs to be applied to this system [24]. This results in the following:

1. The variable *A* accounts for the deterioration in inelastic performance of CBF with increasing brace slenderness. The expression for the variable is shown by Eq. (3) where "α/c" is the post-buckling compression capacity of the brace.

For the case of the RSFJ tension-only brace, because there is no buckling in the braces and the capacity of the braces is only related to the devices (which are deigned based on the demand), the α/c can be taken as 1.0. Therefore, the variable *A* will be taken as 1.0 when designing the RSFJ tension-only braces.

$$A = 1/[0.5(1 + \alpha_c^{/})] \quad (3)$$

Note the device itself is elastic and both the non-sliding (before F_{slip}) and sliding phases and hysteretic performance of the device are stable and repeatable [19].

2. The variable *B* accounts for the departure of the CBF system from the optimum weak beam-strong column (overall) mechanism towards the less desirable strong beam-weak column (shear) mechanism. This can be due to less than ideal hysteretic behaviour of the CBF system [25]. In the standard, this variable is storey-dependent and is expressed as a function of the height of the building compared with the maximum height limit (from Table 12.12.4 in [24]). It ranges from 1.1 for structures under 1/3 of this height limit to 1.3 for structures over 2/3 of the limit. On that basis, the value of for the design example here would be 1.2. However, it can be argued that a well-designed and detailed RSFJ tension-only brace (that has been experimentally proven to have a stable hysteretic) with capacity designed beams and columns will develop a reliable overall mechanism comparable to an eccentrically braced frame that in fact does not require this magnification. Thus, for this case, the variable *B* is taken as 1.0.
3. The variable *C* accounts for the influence of inelastic demand on the system by modifying values of products taken from variables *A* and *B* to specify the C_s factor. For category 1 systems, $C = A*B$ which for the case of RSFJ tension-only brace, $C = 1.0$.

3.2.1.3. Step 3: analyse the frame for the required load cases and load combinations. In this step, the frame is analysed considering different

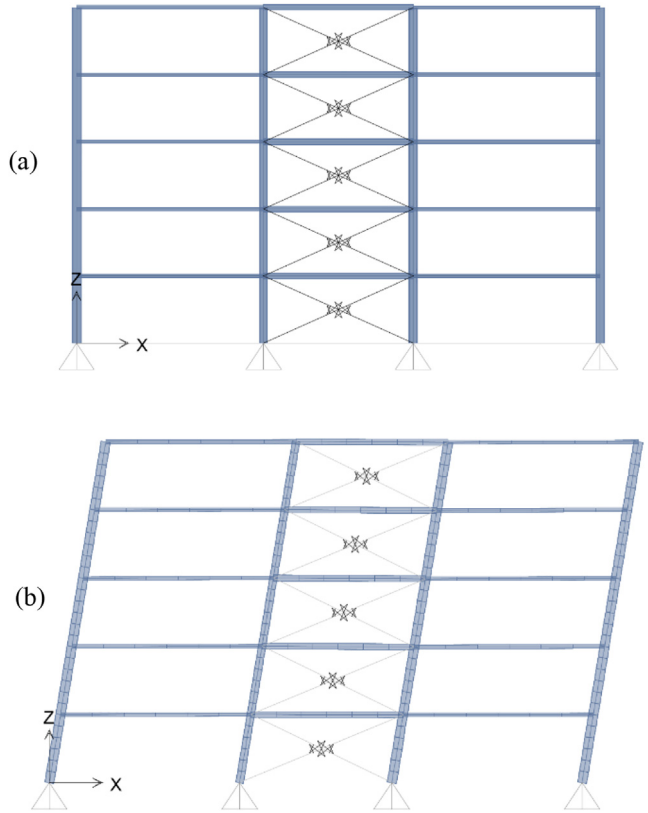

Fig. 4. Numerical model developed for the system: (a) general arrangement (b) deformed shape of the frame.

load cases and combinations. The loads applied during the preliminary design are: a self-weight (for the frame) of 0.8 kPa, a super-imposed dead load of 0.5 kPa, a floor weight of 3 kPa, a cladding weight of 0.8 kPa, a floor live load of 3 kPa and a roof live load of 0.25 kPa. The seismic weight applicable to each braced frame is accordingly calculated as 11,437 kN.

Note that, in order to avoid the design actions on the secondary elements of the seismic resisting system (i.e. those elements suppressed from inelastic demand through the capacity design process; in this case the collector beams and the columns), the design procedure includes calculation of upper limit actions for member and connection strength, stipulated in the standard (Clause 12.9.1.3 of [24]) and denoted by E_{max}. In principle, these actions are just as applicable to this tension only RSFJ system as they are to every other capacity designed seismic resisting system. However, with the closely designed properties of the RSFJ in the non-sliding and the sliding range (behaviour in the sliding range is also elastic) and with the sliding range extended out to 1.25x the ULS design deformation limits (as per the experimental results related to the RSFJ secondary fuse action [29]), the upper limit actions will always be greater than the capacity design derived design actions based on overstrength. This also is confirmed by the previous experimental results and is further investigated by nonlinear dynamic time-history simulations at the last section of this paper.

The ESM method or RSA method [26] can be used to calculate the base shear of the structure; in the design example presented herein the ESM method is used. For preliminary design, the fundamental period of the structure is calculated using the empirical formula given in the [26] (and is equal to 0.54 s). Note that this value will later be verified by modal analysis.

A ductility factor of $\mu = 3.0$ and a structural performance factor of $S_p = 0.7$ are adopted for the design. Note that the ductility selected here could be conservative and it is recommended to verify this factor by nonlinear dynamic time-history simulations later to efficiently size the RSFJs and the rest of the structure, although for a typical design that would be much more design effort than is routinely used or needed. The structural performance factor (S_p) is proposed in the standard ([26]) to account for the effects that cannot directly be measured and not explicitly included in the analysis. Some of these effects are: typically stronger than predicted structural members due to higher material strength and strain hardening, redundancy in the structural components, energy dissipation from secondary-structural elements and also from the foundation.

It is recommended that S_p value should be taken as 0.7 for structural ductility factors more than 2.0 [26]. On this basis, the storey shears have been determined as 2739 kN, 2563 kN, 2211 kN, 1683 kN and 978 kN for the level 1 to roof, respectively. Di Lauro et al. [30] provided a comprehensive study on the appropriate over-strength coefficient and safety factors applicable to friction connections. The aim is to keep the main structural members in the elastic range while friction devices deform [31]. For the RSFJ system, there is a built-in collapse-prevention secondary fuse which will be activated when the applied load to the brace is larger than the design load. The device can provide 50% displacement more than the design displacement, while the force in the device will increase by a factor of 1.25. Thus, an over-strength factor of 1.25 is used to design the brace body and the collector beams while an over-strength factor of 1.5 is used to capacity design the columns. Note that a safety factor of $\varnothing = 0.8$ is used for the design of the capacity-protected members. Also, the demand-to-capacity ratio for these members was less than 0.8. The reader is referred to [29] for more information about the secondary fuse including experimental results and design equations.

3.2.1.4. Step 4: assess P-delta effects and check the seismic lateral deflections. A structural analysis in the SAP2000 [32] program is performed in this step to evaluate the P-delta effects and to check the seismic lateral drifts. A 2D model of one of the braced frames was considered for modelling. The beam to column connections and the base connections are considered as pinned joints while the column sections are continuous as required by [26]. A rigid diaphragm has been assigned to each floor to represent the effect of floor slabs and to ensure that each node in a same floor experience a same lateral deflection. The gravity loads have been assigned to the beams. The seismic weights have also assigned to the nodes in each elevation. Fig. 4 shows the general arrangement of the model.

The design approach taken was that the structure remains linear elastic under Serviceability Limit State (SLS) level events and the maximum lateral inter-story under Ultimate Limit State (ULS) level is limited to 2%. Note that the standard allows for a maximum inter-storey drift of 2.5%, however, according to the observations after the Christchurch Earthquake, lower values are more desirable to minimize the damage in the structure [1]. Flag-shaped responses for the devices were accordingly designed and calibrated (on the basis of the frame undergoing an elastic lateral drift of 0.3% before opening the joints). Based on the ductility factor adopted for the design ($\mu = 3.0$), F_{slip} was assumed as 70% of $F_{ult,loading}$ for all RSFJs so satisfy the SLS drift criteria. In fact, the drift limit states (0.3% at SLS and 2% at ULS) indicated the post-slip stiffness (stiffness of the system after the devices are activated) of the system. The seismic performance of the system is further investigated in the last section of this paper.

The RSFJs are modelled using the “Damper – Friction Spring” link element with the “tension-only” feature activated. The initial stiffness of the links is considered as the elastic stiffness of the brace body after running the analysis and optimising the model. Table 1 shows the hysteretic properties of the RSFJs.

In order to numerically model the RSFJ in SAP2000 software package, the numerical parameters of the ‘Damper-Friction Spring’ link elements need to be calibrated to represent the flag-shape load-deformation response of the RSFJs. Table 2 shows the calibrated parameters for the tension-only braces. The accuracy of this method for

Table 1
Hysteretic properties of the RSFJ braces.

Level	Roof	4	3	2	1
Parameter	RSFJ5	RSFJ4	RSFJ3	RSFJ2	RSFJ1
F_{slip} (kN)	753	1294	1700	1971	2107
$F_{ult,loading}$ (kN)	1075	1849	2429	2816	3010
$F_{ult,unloading}$ (kN)	375	647	850	985	1055
$F_{residual}$ (kN)	108	185	243	281	301
Δ_{max} (mm)	56	56	56	56	56

Table 2
Input parameters for the numerical modelling of the RSFJs.

Level	Roof	4	3	2	1
Parameter	RSFJ5	RSFJ4	RSFJ3	RSFJ2	RSFJ1
$K_{loading}$ (kN/mm)	5.75	9.9	13.00	15.09	16.13
$K_{unloading}$ (kN/mm)	4.76	8.25	10.83	12.57	13.46
Maximum displacement (mm)	56	56	56	56	56
Pre-compression displacement (mm)	−130	−130	−130	−130	−130

modelling of RSFJs has been verified before. The reader is referred to [22] for more information about calibrating of the link element including the calibration methods, numerical results and discussions.

As mentioned, Fig. 4 shows the configuration of the model and the deformed shape of the structure. The fundamental period of the structure from the model is 0.55 s that is consistent with the previous calculated value (0.54 s). The earthquake-induced deflections of the structure are majorly controlled by the RSFJs and for all storeys, the inter-storey drift was reasonably close to 2% which is in fact the design target. In addition to the displacement found from the analysis, the standard also considers the increase in displacements due to P-delta effects. These effects, however, are not required for this case study respecting the clause 6.5.2(c) of [32]. The analyses have shown that the stability coefficients (θ) calculated using Eq. (4) are less than 0.1 for all the storeys, which is expected for a CBF system. In Eq. (4), W_i is the seismic weight of the storey, (h_i-h_{i-1}) is the storey height, δ_{ui} is the ULS storey displacement and V_i is the storey shear strength (conservatively can be taken as the design storey seismic force). Given that the calculated value for all levels was less than 0.1, the P-delta effects is insignificant and not considered in the actions [26].

$$\theta = \frac{W_i \delta_{ui}}{V_i (h_i - h_{i-1})} \tag{4}$$

3.2.2. Structural member design

3.2.2.1. Step 5: determine the required brace member sizes. In this step, the brace member sizes are determined. For the tension-only x-braces, any element that can resist tension loads can be used. For this structure, non-threaded rods of grade 830 MPa were considered and designed with an over-strength factor of 1.25 on the force associated with full expansion of the RSFJs as described in Step 3 of the procedure. Fig. 5 shows the performance of a system with RSFJs as lateral load resisting members. As mentioned, the behaviour of the RSFJ secondary fuse and the associated over-strength mechanism are experimentally demonstrated. The reader is referred to [29] for more information including results and discussions.

As can be seen in the figure, before activation of the secondary fuse, the system is elastic with a geometrically non-linear behaviour provided by the RSFJs. When the applied load is higher than the design load, the secondary fuse is activated and the system produces extra resistance up to 1.25 times of the design load. The extra deflection provided by this feature is 1.5 times of the design displacement. After secondary fuse, the system still has a flag-shaped load-deformation response with a self-centring behaviour and there will be no slack in the tension-only members.

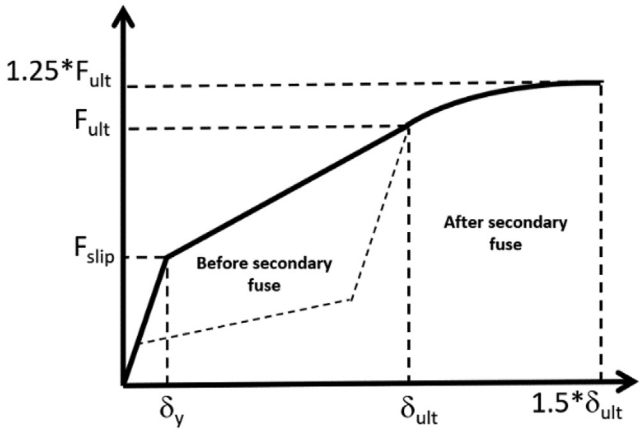

Fig. 5. RSFJ system performance with secondary fuse.

As per [25] for tensioned braced CBFs, the forces due to gravity loads are usually negligible and the braces are designed only for seismic loads. The diameter of the rods is therefore specified as 80 mm, 75 mm, 70 mm, 60 mm and 50 mm for level 1 to roof, respectively. Note that instead of one rod, using even number of smaller in size rods (similar to the detail shown in Fig. 2) may be more practical in real cases.

3.2.2.2. Step 6: calculate the brace over-strength tension capacities. This step implements the capacity design procedures where all other structural members are designed for the capacity-design derived actions from the RSFJs to ensure that the chosen ductile failure mechanism develops. Reference [25] suggests the following equation:

$$N_{brace}^{ot} = \varnothing_{oms} A_g f_y \tag{5}$$

where N_{brace}^{ot} is the brace over-strength tension capacity, $\varnothing_{oms}$ is the appropriate over-strength factor used to size the non-yielding element (for the case of the RSFJ tension-only brace, the brace body and the attachments) and A_g is gross area of the cross section. As mentioned in Step 3 and Step 5, an over-strength factor of $\varnothing_{oms} = 1.25$ is suggested for this case respecting the experimental tests described in [29]. Note that it is very unlikely for the RSFJ to develop a more than expected resistance (based on extensive testing on these devices reported in [19,29,33]). Nevertheless, it is the designer's choice to make allowances to account for greater than specified strength of the material.

3.2.2.3. Step 7: determine the collector beam capacity design derived actions. The collector beams at each level are subjected to axial compression forces (due to the transfer of horizontal component of the brace tension force from the floor above to the floor below) and the shear/bending actions from the gravity loads. The collector beam capacity design derived seismic compression force can be determined using Eq. (6):

$$N_{beam,i}^{c} = N_{brace,i}^{ot} \cos\theta_i \tag{6}$$

where N_{brace}^{ot} is calculated using Eq. (5) and θ_i is the angle between the brace at level i and the beam (24 degrees for this structure). The shear and bending actions are calculated assuming simply supported boundary conditions for the beams. The design of the beams was governed by the combined actions of axial forces and bending moments.

3.2.2.4. Step 8: determine the column capacity design derived actions and design actions. The capacity design seismic compression and tension forces are determined using Eqs. (7) and (8):

$$N_{col,i,com}^{c} = \sum_{i}^{n} N_{brace,i}^{ot} \sin\theta_i \tag{7}$$

$$N^{c}_{col,i,ten} = \sum_{i+1}^{n} (N^{ot}_{brace}\sin\theta_i)_{i+1} \quad (8)$$

where '*n*' is the level at the top of the CBF (bracing for this case) system. The column seismic axial forces are combined with the compression forces for the gravity load combination considering the appropriate sign. When column seismic tension force exceeds the column gravity compression force, the column design tension force is negative indicating that the column is subjected to net uplift. This was not the case for this structure.

The column design bending moments usually results from the eccentric beam shear force (eccentric beam shear force relative to the column centreline) and the nodding eccentricity (the eccentricity between the axial force in the brace and the column centreline). Wijanto [28] suggest the moment resulted from these eccentricities are not considerable thus they are neglected for this case study structure.

3.2.2.5. Step 9 and step 10: design the collector beams and columns. The beams and columns are designed based on the capacity design actions derived from previous steps. Standard Universal Beams (UB) and Universal Column (UC) sections are considered for the collector beams and columns, respectively. As mentioned earlier, the capacity design over-strength factor applied to the columns is 1.5. The columns were kept continues up the height of the structure.

The specified sections were then assigned to the members in the numerical model. Fig. 6 shows the designed sections following Step 7 to Step 10 of the procedure. Note that given the pinned connections for the beams, braces and column bases, the system level seismic performance is mostly governed by the characteristics of the braces.

3.2.2.6. Step 11: design and detail the connections. Designing and detailing of the connections should be properly done using the appropriate over-strength factors. For the RSFJ tension-only braces, an example of connection detailing concept is illustrated in Fig. 2. As mentioned, based on the performance of the RSFJ secondary fuse [29], a minimum over-strength factor of 1.25 is recommended for designing the pins, connections and other attachments.

4. Non-linear static pushover and non-linear dynamic time-history analyses

In this section, non-linear static pushover and non-linear dynamic time-history analyses are performed on the designed structure to investigate the global seismic performance of the system and verify the proposed design procedure. 10 earthquake records are used for the simulations [34]. The record are scaled for ULS based on the method described in [26] for the given location and soil type. In addition to the time-history analyses, a nonlinear static pushover analysis was performed to verify the intended performance of the system that is originating from the RSFJ tension-only braces. Fig. 7 shows the pushover curve. A monitored-displacement approach was used to perform this analysis. The displacement at the roof is monitored up to the target drift limit (2%).

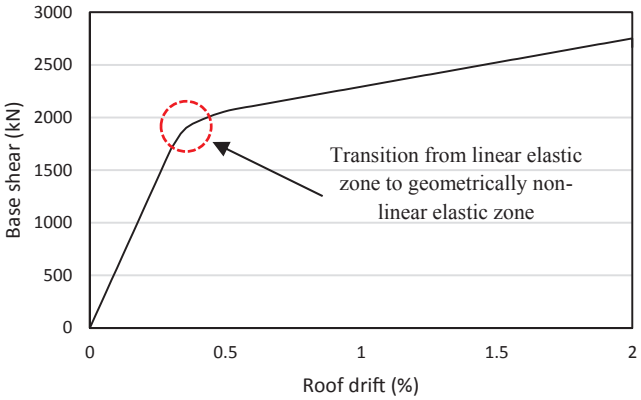

Fig. 7. Results of non-linear static pushover analysis.

As can be seen, the base shear of the structure at 2% of roof lateral drift matches the base shear calculated from ESM. The structure shows a bi-directional performance resulting from the flag-shape hysteresis of the RSFJ tension-only braces.

It can be seen in the graph that the structure remains linear elastic (RSFJs are not activated) up to 0.3% of lateral drift which in fact was one of the performance targets of the design. After this point, the RSFJs start to activate resulting in the observed bi-linear pushover curve. Note that since not all RSFJs are activated at the same time, a transition zone from the linear elastic zone to the geometrically nonlinear zone is observable in the pushover curve. Even in the transition zone, the structure as a whole is elastic, and no material nonlinearity is expected. Note that in order to verify that the columns remained in their elastic range, in the numerical model, plastic hinges were assigned up the height of the columns and as expected, no inelastic behaviour was observed. This was also expected considering that the capacity design procedure followed for this structure has been proven to be an effective method to retain the columns in the elastic state under actual severe earthquakes [1].

Fig. 8 shows the scaled records versus the target design spectra. Note that for time-history simulations, the RSFJs are allowed to continue expanding up to 1.5 times of the ULS design deflection to account for the effect of the secondary fuse.

The New Zealand standard [26] requires a family of not less than

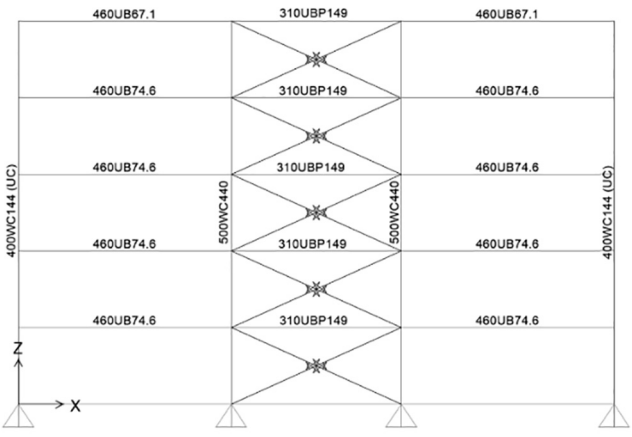

Fig. 6. Sections assigned.

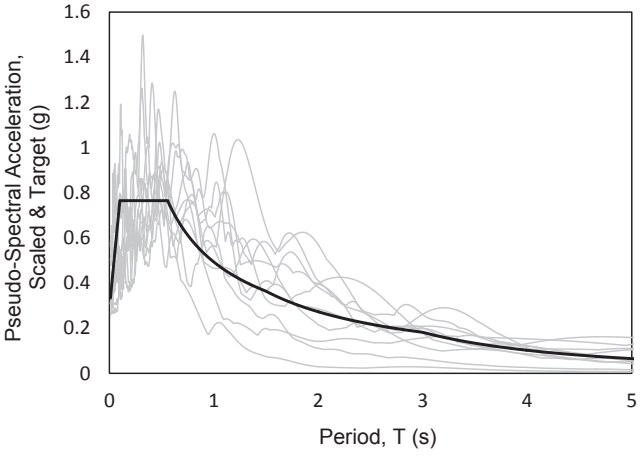

Fig. 8. Scaled and target spectrums.

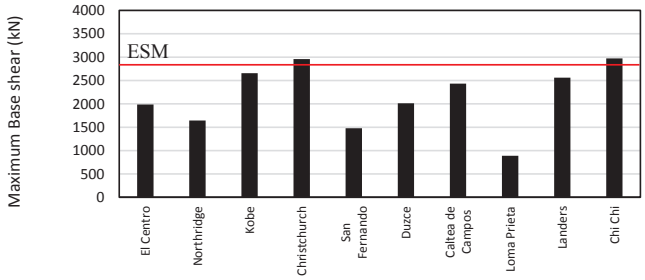

Fig. 9. Maximum base shears.

three records for time-history analysis. Also it is mentioned that the most critical value on the response parameters across the family has to be used to determine the acceptability of the analysis. On the other hand, the majority of other international codes [35–37] consider "peak of three" or the "average of seven" as acceptable and emphasizes that if less than seven records are chosen for the analyses, the maximum response must be used. According to Bradley [34], the maximum of three or the mean of seven can conservative and unconservative, respectively. Thus, in this paper, ten records are used and a mixed approach from the abovementioned approaches is taken to interpret the results of the time-history analyses.

Fig. 9 shows the maximum recorded base shears for the chosen seismic events. It can be seen that the average base shear of the ten simulations is 2159 kN which is lower than the base shear from the ESM (2739 kN). The highest recorded base shears are related to the Christchurch event (2958 kN) and Chi Chi event (2972 kN) which are slightly higher than the target base shear. The latter is the maximum of all records. Note that if the average base shear of the records is taken, it is well below the design base shear which confirms the acceptable seismic performance. If the maximum of all records is considered (which as discussed can be overly conservative), it is slightly above the design base shear. However, owing to the secondary fuse over-strength function of the devices, the structure can tolerate up 1.25 times of the design base shear without any damage except yielding of the clamping rods in the RSFJs (see Fig. 5). This also verifies the efficiency of the seismic design.

Fig. 10 shows the peak roof drifts. As can be seen, the average top lateral drift is 1.16% and the largest recorded drifts are for the Christchurch event (2.12%) and Chi Chi event (2.17%). If the mean of the recorded drifts is considered, it is well below the target drift (2%) and this confirms the acceptable seismic performance of the designed structure. If the maximum of all records is considered (which could be very conservative), it is slightly above the design base shear. Nevertheless, because of the secondary fuse over-strength function of the devices, the structure can tolerate up 1.5 times of the design drift without any damage except yielding of the clamping rods in the RSFJs (see Fig. 5). This also confirms the efficiency of the seismic design conducted.

Note that capacity of the structural members (shown in Fig. 7) was

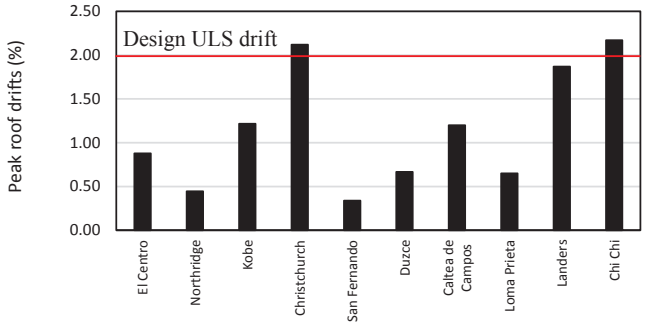

Fig. 10. Peak roof drifts.

checked for all of the time-history load cases and they were sufficient. This also confirmed the fact that there was no unexpected upper limit demand on the structural members (rather than devices) so not considering the upper limit effect is step 2 of the procedure was close to reality.

Fig. 11 shows the roof displacement histories for four of the analysed cases as representatives for all cases. As can be seen in the figure, no significant residual displacement was recorded at the end of the events. For some of the observed records, the structure was oscillating towards the end of the event. Nevertheless, the amplitude of those displacement was less than 0.05% lateral drift which can be neglected. This observed self-centring behaviour on the system level can be attributed to the flag-shape load deformation response of the tension-only braces. Fig. 12 depicts the load-deformation response of the RSFJ tension-only braces at the first floor for the four mentioned analyses cases. It can be seen in the figure that the braces performed well within the expected specifications and the link elements could successfully represent the behaviour of the RSFJs.

In summary, the results of the time-history simulations demonstrated that the structure was able to meet the force and displacement demands. More to the point, it is demonstrated that the structure is properly designed and the RSFJ braces are properly sized.

4.1. Further discussion on the adopted C_s factor

As mentioned in Step 2 of the proposed procedure, a $C_s = 1.0$ is assumed for the structure with RSFJ tension-only braces. The results of the non-linear dynamic time-history simulations showed that the structural members remain linear elastic for all load cases while the inelastic behaviour of the system was the result of the geometrically nonlinear performance of the links (RSFJs). Therefore, it can be concluded that the presented numerical results support the use of the *Cs* factor adopted for this case study. Nevertheless, one can argue that more comprehensive time-history simulations on different types of structures with different number of stories may be required to generalise the use of lower C_s factors for RSFJ tension-only braces. In this case, a conservative approach is to use more conservative C_s factors related to variable *B*.

As mentioned in step 2 of the procedure, variable *B* accounts for departure of the system from optimum o-mechanism (weak beam-strong column) to the s-mechanism (strong beam-weak column). This is usually suppressed by the capacity design requirements by the columns and locating the column splices away from the floor to keep the column effective continuity up the height. This value is then story dependent and should be 1.1 for structures up to 1/3 of the maximum height limitations indicated in clause 12.12.4 of [24], 1.2 for structures between 1/3 and 2/3 of this limit and 1.3 for structure higher than 2/3 of this limit. For example, for the case study structure presented, B = 1.2 can be used given the applicable height limitation discussed in step 1 of the procedure. This would lead to a more conservative $C_s = 1.2$ factor for the design.

5. Conclusions

This paper proposes a step-by-step design procedure for steel structures with diagonal Resilient Slip Friction Joint (RSFJ) braces effective in tension only. The RSFJ is a friction-based energy dissipation device that can provide damping and self-centring behaviour in one package resulting in a flag-shaped hysteresis. The paper also discussed that the code-prescribed height limitations and C_s factors for conventional tension-only braces may not apply for the RSFJ tension only brace.

The proposed procedure is used to design a 5-storey steel structure with RSFJ tension-only braces followed by non-linear static pushover analysis and non-linear dynamic time-history simulations. The results confirmed the efficiency of the proposed design procedure for designing

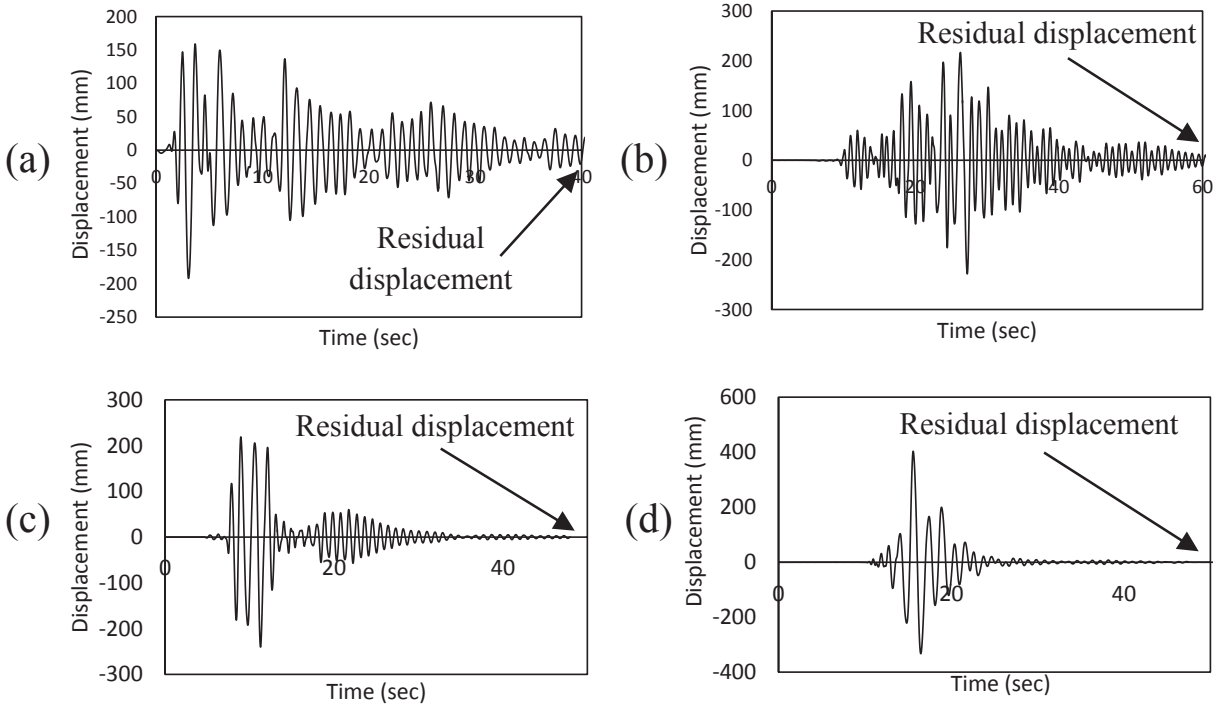

Fig. 11. Roof displacement histories: (a) El Centro (b) Caltea de Campus (c) Kobe (d) Christchurch.

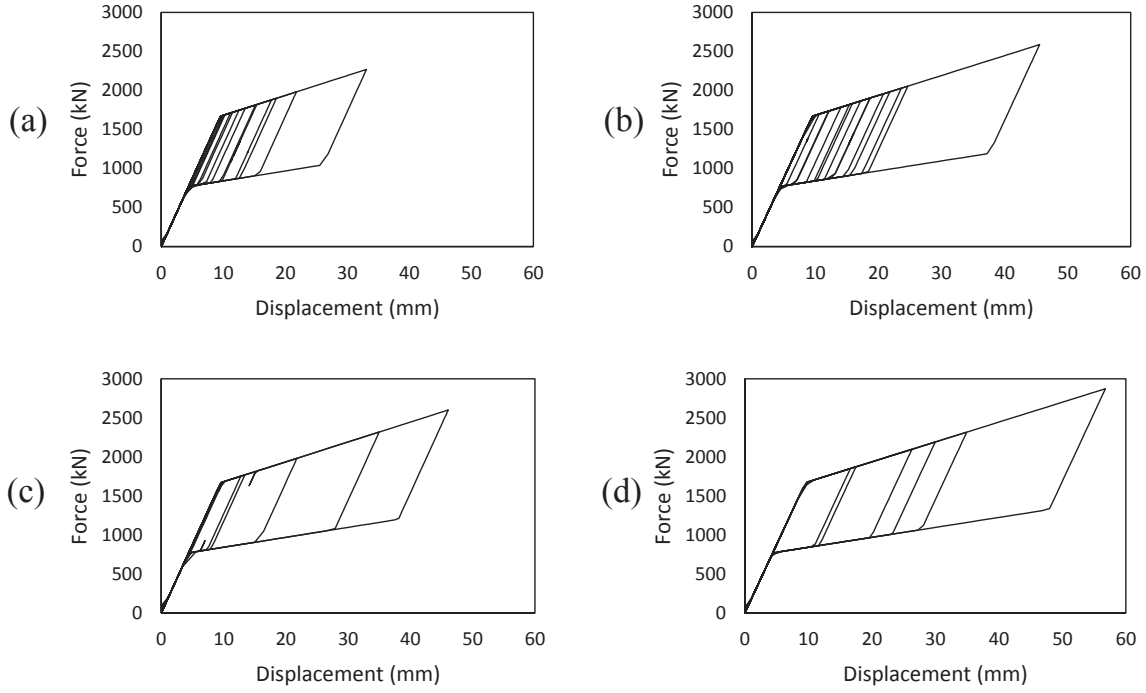

Fig. 12. Response of the link elements modelling the RSFJ tension-only braces: (a) El Centro (b) Caltea de Campus (c) Kobe (d) Christchurch.

the structure and sizing the devices. This procedure can also be used for other low damage bracing systems that have a flag-shaped hysteresis. Future research can be involved with applying the procedure to other systems with flag-shaped response and verifying it by time-history analysis. Also, further experimental studies can be conducted to evaluate the over-strength and safety factors applicable to the device itself that includes the effects of friction property and variation in clamping bolts preload.

Declaration of Competing Interest

The authors declare that they have no known competing financial interests or personal relationships that could have appeared to influence the work reported in this paper.

Acknowledgement

The authors would like to thank Ministry of Business, Innovation and Employment (MBIE) of New Zealand for the financial support of

this research.

References

[1] Bruneau M, MacRae G. Reconstructing christchurch: a seismic shift in building structural systems. Quake Cent. Report, Univ. Canterbury, Christchurch, New Zeal.. 2017.
[2] Bruneau M, Clifton C, MacRae GA, Leon R, Fussell A. Steel Building damage from the Christchurch earthquake of February 22, 2011. Bull New Zeal Soc Earthq Eng 2011;44(4):297–318.
[3] McCormick J, Aburano H, Ikenaga M, Nakashima M. "Permissible residual deformation levels for building structures considering both safety and human elements. Proceedings of the 14th world conference on earthquake engineering. 2008. p. 12–7.
[4] Pall AS, Marsh C, Fazio P. Friction joints for seismic control of large panel structures. PCI J 1980;25(6):38–61.
[5] Baktash P, Marsh C, Pall A. Seismic tests on a model shear wall with friction joints. Can J Civ Eng 1983;10(1):52–9.
[6] Pall AS, Marsh C. Response of friction damped braced frames. J Struct Eng 1982;108(9):1313–23.
[7] Popov EP, Grigorian CE, Yang T-S. Developments in seismic structural analysis and design. Eng Struct 1995;17(3):187–97.
[8] Clifton GC, MacRae GA, Mackinven H, Pampanin S, Butterworth J. Sliding hinge joints and subassemblies for steel moment frames. Palmerston North, New Zealand: Proc of New Zealand Society for Earthq Eng Conf. 2007.
[9] Bora C, Oliva MG, Nakaki SD, Becker R. Development of a precast concrete shear-wall system requiring special code acceptance. PCI J 2007;52(1):122.
[10] Loo WY, Kun C, Quenneville P, Chouw N. Experimental testing of a rocking timber shear wall with slip-friction connectors. Earthq Eng Struct Dyn 2014;43(11):1621–39.
[11] Dal Lago B, Biondini F, Toniolo G. Friction-based dissipative devices for precast concrete panels. Eng Struct 2017;147:356–71.
[12] Hashemi A, Masoudnia R, Quenneville P. A numerical study of coupled timber walls with slip friction damping devices. Constr Build Mater 2016;121:373–85.
[13] Hashemi A, Masoudnia R, Quenneville P. Seismic performance of hybrid self-centring steel-timber rocking core walls with slip friction connections. J Constr Steel Res 2016;126:201–13.
[14] Loo WY, Quenneville P, Chouw N. A numerical study of the seismic behaviour of timber shear walls with slip friction connectors. Eng Struct 2012;34:233–43.
[15] Iyama J, Seo CY, Ricles JM, Sause R. Self-centering MRFs with bottom flange friction devices under earthquake loading. J Constr Steel Res 2009;65(2):314–25.
[16] Wolski M, Ricles JM, Sause R. Experimental study of a self-centering beam–column connection with bottom flange friction device. J Struct Eng 2009;135(5):479–88.
[17] Lin Y-C, Sause R, Ricles JM. Seismic performance of steel self-centering, moment-resisting frame: Hybrid simulations under design basis earthquake. J Struct Eng 2013;139(11):1823–32.
[18] Zarnani P, Quenneville P. "A Resilient Slip Friction Joint," 2015. Patent No. WO2016185432A1, NZ IP Office.
[19] Hashemi A, Zarnani P, Masoudnia R, Quenneville P. Experimental testing of rocking Cross Laminated Timber (CLT) walls with Resilient Slip Friction (RSF) joints. J Struct Eng 2017;144(1).
[20] Hashemi A, Zarnani P, Masoudnia R, Quenneville P. Seismic resilient lateral load resisting system for timber structures. Constr Build Mater 2017;149:432–43.
[21] Hashemi A, Zarnani P, Masoudnia R, Quenneville P. Seismic resistant rocking coupled walls with innovative Resilient Slip Friction (RSF) joints. J Constr Steel Res 2017;129:215–26.
[22] Hashemi A. Seismic resilient multi-story timber structures with passive damping. New Zealand: University of Auckland; 2017.
[23] Bagheri Mehdi Abadi H, Hashemi A, Yousef-Beik SMM, Zarnani P, Quenneville P. Experimental test of a new self-centring tension-only brace using the Resilient Slip Friction Joint. Pacific Conf. Earthquke Eng. (PCEE2019), Auckland, New Zeal.. 2019.
[24] New Zealand Standards, "Steel Structures Standards (NZS 3404: Part 1 and 2)," Stand. New Zealand, Wellingt., 2007.
[25] Feeney MJ, Clifton GC. "Seismic Design Procedures for Steel Structures including Tips on Seismic Design of Steel Structures, " New Zealand Heavy Engineering Research Association Report, Manukau City, New Zealand, 2001.
[26] New Zealand Standards, "Structural Design Actions (NZS 1170.5)," Wellington, New Zeal., 2004.
[27] Hashemi A, Zarnani P, Masoudnia R, Quenneville P. Seismic resilient lateral load resisting system for timber structures. Constr Build Mater 2017;149.
[28] Wijanto S. "Behaviour and design of generic buckling restrained brace systems," no. February 2012, p. 199, 2012.
[29] Hashemi A, et al. Seismic performance of a damage avoidance self-centring brace with collapse prevention mechanism. J Constr Steel Res 2019;155:273–85.
[30] Di Lauro F, Montuori R, Nastri E, Piluso V. Partial safety factors and overstrength coefficient evaluation for the design of connections equipped with friction dampers. Eng Struct 2019;178(April 2018):645–55.
[31] Piluso V, Montuori R, Nastri E, Paciello A. Seismic response of MRF-CBF dual systems equipped with low damage friction connections. J Constr Steel Res 2019;154:263–77.
[32] Computers and Structures, "SAP2000 Ver. 19 (2017)." Berkeley, CA, 2017.
[33] Hashemi A, Zarnani P, Masoudnia R, Quenneville P. Seismic resistant rocking coupled walls with innovative Resilient Slip Friction (RSF) joints. J Constr Steel Res 2017;129.
[34] Bradley BA. Seismic performance criteria based on response history analysis: alternative metrics for practical application in Nz. Bull New Zeal Soc Earthq Eng 2014;47(3):1–5.
[35] Eurocode Standards, "Eurocode 8: Design of structures for earthquake resistance-part 1: general rules, seismic actions and rules for buildings," 2005.
[36] B. S. S. Council, "National Earthquake Hazards Reduction Program (NEHRP) Part 1: Recommended Provisions for seismic regulations for new buildings and other structures, 2000 Edition (FEMA 368)," In: Prep. by Build. Seism. Saf. Counc. Fed. Emerg. Manag. Agency, Washingt. DC, 2000.
[37] Merritt FS. Minimum design loads for buildings and other structures: American Society of Civil Engineers Standard 7–95. J Archit Eng 1996;2(2):80–1.